PHYSICAL REVIEW B VOLUME 56, NUMBER 4 15 JULY 1997-II

Photoelectron spectroscopic investigation of the bias-enhanced nucleation of polycrystalline diamond films

P. Reinke and P. Oelhafen
Universität Basel, Institut für Physik, Klingelbergstrasse 82, 4056 Basel, Switzerland

(Received 25 March 1997)

In the present work we describe an investigation of the nucleation mechanism of polycrystalline diamond films if the bias-enhanced-nucleation (BEN) method is used. Photoelectron spectroscopy with excitation energies in the ultraviolet [ultraviolet photoelectron spectroscopy (UPS)] and x-ray regime (x-ray photoelectron spectroscopy) as well as electron energy loss spectroscopy are employed to monitor the nucleation process and the subsequent diamond film growth. The deposition is performed *in situ*, thus avoiding surface contamination with oxygen or hydrocarbons. The observation of the temporal evolution of composition and structure of the deposited film and its interface with the underlying silicon substrate allow us to develop a qualitative model, which describes the nucleation process. The BEN pretreatment leads, through the irradiation with low-energy ions, to the codeposition of an amorphous carbon phase and the crystalline diamond phase. The presence of both phases is readily apparent in the UPS analysis, which will prove to be an indispensible tool in the structural characterization of the carbon phase present at the surface. There is no indication for the presence of graphite or large graphitic clusters. A deconvolution of the C 1*s* and Si 2*p* core-level peaks does confirm the presence of two carbon phases and the formation of a silicon carbide interface. With increasing deposition time the contribution of diamond to the carbon film increases and upon switching to diamond growth conditions the amorphous carbon phase is rapidly etched and only the diamond crystals remain and continue to grow. This removal of the amorphous phase leads to a decrease in the overall carbon concentration at the surface by 18–30 % during the first 30 sec of the diamond growth period and was observed for a variety of pretreatment conditions. A silicon carbide interfacial layer is formed early on during the BEN pretreatment and its thickness is reduced considerably by etching during the diamond growth period. These results are summarized and discussed in the framework of a qualitative model for the nucleation process. [S0163-1829(97)03628-X]

INTRODUCTION

For a long time the extreme properties of diamond have sparked interest in its use for technical applications apart from the admiration of its beauty as a gemstone. But only the development of techniques to synthesize diamond and polycrystalline diamond films has allowed us to take advantage of the exceptional properties of this material. The advances made in the last few years with respect to the texture control and high rate deposition of diamond films provide the means to produce, for example, diamond windows of high optical quality. A prerequisite for the growth of a polycrystalline diamond film is a pretreatment of the substrate in order to provide a surface structure and composition which favors diamond nucleation.[1] The most frequently applied methods are an abrasion of the surface with a diamond paste, which is a purely mechanical pretreatment, and the newly developed bias-enhanced nucleation (BEN).[2–4] The BEN method is advantageous in several respects. It is a nondestructive *in situ* method which leads to a high nucleation density and favors under certain deposition conditions the formation of nearly heteroepitaxial diamond films on Si.[2,5,6] The BEN method involves the irradiation of the substrate with low-energy ions which is usually achieved through the application of a dc voltage to the substrate. The estimates for the ion energies range from 30 to 150 eV, which results in a rather shallow penetration depth of at most 2–3 monolayers.[7–9] As an alternative for insulating substrates, such as ceramics or quartz, the application of a rf bias voltage can be envisaged.[10] Apart from the technical challenges of the BEN method the questions which have to be dealt with now concern the mechanism or reaction pathways by which BEN proceeds. Or in other words, why does the BEN pretreatment prior to the diamond growth process itself provide such a favorable environment for the nucleation of diamond as opposed to the diamond nucleation on an untreated Si or SiC substrate? This question has been central to a number of recent publications and different models have been proposed to describe the nucleation mechanism in BEN.[3,4,11–14] The presence of a carbon phase different from diamond such as graphite,[14] tetrahedral amorphous carbon (ta-C),[7] or sp^2 amorphous carbon has been suggested to play an important role in promoting diamond nucleation, especially during BEN. However, most analytical methods frequently employed in the study of diamond growth and nucleation are not sensitive to thin layers of noncrystalline or graphitic material formed at the substrate surface prior to or during the early stages of crystal growth. It was already demonstrated by Belton and Schmieg[15] that surface-sensitive methods such as x-ray photoelectron spectroscopy (XPS) or electron energy loss spectroscopy (EELS) can be applied successfully to study diamond growth on different substrate materials. But Belton and Schmieg also pointed out that XPS alone is not sufficient to characterize the structure of the carbonaceous deposit and has to be supplemented by other methods.

In order to contribute to the development of a better understanding of the nucleation process we combined the depo-

0163-1829/97/56(4)/2183(8)/$10.00

sition of diamond films using BEN with the subsequent analysis of the deposit with photoelectron spectroscopy. Photoelectron spectroscopy (PES), with excitation energies in the ultraviolet [ultraviolet photoemission spectroscopy (UPS)] and x-ray regime, allows the determination of the electronic structure which is closely connected to the local coordination and chemical environment of the carbon atoms and therefore sensitive to changes in the matrix structure itself.[16–18] It also allows, due to its surface sensitivity, monitoring of the interface formation between the substrate and the growing film and has been applied successfully to investigate the interface formation between amorphous hydrogenated carbon and a variety of substrate materials.[19] A prerequisite for the experiment is the *in situ* deposition of the diamond film, which is transferred from the microwave (MW) deposition reactor to the PES-analysis chamber without breaking the vacuum. Although it is well known that the diamond surface itself is stable in air for several weeks, this is in our experience not valid for the interface and other intermediate components formed in the course of the deposition process.

Our experiment to study the BEN nucleation mechanism involves the observation of the temporal evolution of the film structure and chemical composition in the course of the BEN pretreatment step and the subsequent diamond growth. The information which can be deduced from the PES experiment allows us to develop a qualitative model for film growth and structure during BEN and its influence on the diamond film growth.

EXPERIMENT

The experiment was performed in a vacuum system which consists of two interconnected units: the microwave deposition reactor and the vacuum chamber where the photoelectron spectroscopic analysis is performed. This setup allows us to transfer the samples from the deposition to the analysis chamber without breaking the vacuum and the surface contamination can therefore be minimized. A carbon film as it is produced after a few minutes of BEN shows after only brief exposure to air an oxygen concentration of at least 10%, rendering the following analysis doubtful. Apart from the reaction of the film or interfacial layer with oxygen the exposure to air and adsorption of other contaminants is detrimental to the very surface-sensitive UPS.

The microwave reactor consists of a quartz tube with a diameter of 5 cm which intersects a microwave waveguide (2.45 GHz). The molybdenum substrate holder is electrically grounded and an additional circular tungsten wire serves as anode during the BEN pretreatment. The gas flow is regulated by calibrated mass flow controllers and the base pressure is in the 10^{-7}-mbar range. The temperature of the Si(100) substrate was adjusted via the microwave input power and monitored by a one color optical pyrometer. The deposition parameters throughout the experiment were chosen as follows: a microwave input power of 630–650 W and a substrate temperature of 790–800 °C, the total gas flow was 100 SCCM (SCCM denotes cubic centimeter per minute at STP), and the pressure 40 mbar. For the BEN pretreatment step we chose a mixture of 2.4% methane in hydrogen and a dc-bias voltage of −250 V was applied to the substrate. The methane concentration was reduced to 0.8% and the dc-bias voltage turned off for the diamond growth period. In order to establish stable plasma conditions at the beginning of the deposition and reduce the surface contamination of the substrate, each sample was subjected to a pure hydrogen discharge with the deposition parameters given above for 2 min without and for 2 min with additional dc bias. In addition a few films were deposited using considerably higher methane concentrations of 16.7% (total flow: 96 SCCM), 24% (total flow: 66 SCCM), and 34.8% (total flow: 46 SCCM) during the pretreatment step.

TABLE I. Summary of time intervals after which the deposition was interrupted and the film subsequently analyzed with photoelectron spectroscopy. The labels (A–F, a–e) are used for the identification of spectra in the figures.

BEN pretreatment period		Diamond growth period	
A	3 min	a	30 sec
B	6 min	b	2 min
C	7.5 min	c	5 min
D	9 min	d	10 min
E	12 min	e	15 min
F	15 min		

The film deposition was interrupted after certain time intervals lasting 3–15 min for the pretreatment period and 30 sec–15 min for the subsequent diamond growth step and for each interval a new sample was prepared. The respective deposition intervals are summarized in Table I. After a brief pump down period the samples were transferred to the analysis chamber. We were therefore able to observe the temporal evolution of the film composition and structure during the entire deposition period, which includes the pretreatment and the diamond growth step.

The photoelectron spectroscopy analysis was performed on a Leybold EA11/100 system with a base pressure in the 10^{-10}-mbar range. Monochromatized Al $K\alpha$ (1486.6-eV) radiation was used to record the core-level spectra (MXPS). A helium gas discharge lamp emitting light in the ultraviolet region (He I, $h\nu = 21.22$ eV and He II, $h\nu = 40.82$ eV) was used to determine the valence-band spectra (UPS). The typical resolution was 0.1–0.2 eV for UPS and 0.8 eV for the MXPS measurements. The spectra have been recorded using constant retardation ratio for the UPS and constant pass energy for the MXPS measurements and are presented here without background or satellite subtraction. The energies of the discussed spectral features are given with respect to the Fermi level (E_F) and the Au $4f_{7/2}$ core-level line (positioned at 84.0-eV binding energy) of a clean gold sample.

RESULTS

The temporal evolution of the valence-band spectra (VB spectra) for the BEN pretreatment is depicted in Fig. 1 (He I, He II). The He I spectrum is at the beginning of the BEN (3 min deposition time) period dominated by a broad peak centered at 6.7 eV and a shoulder located between 3.0 and 4.0 eV. With increasing deposition time the main peak is shifted to higher binding energies and the intensity of the shoulder is reduced considerably, while a shoulder located at lower

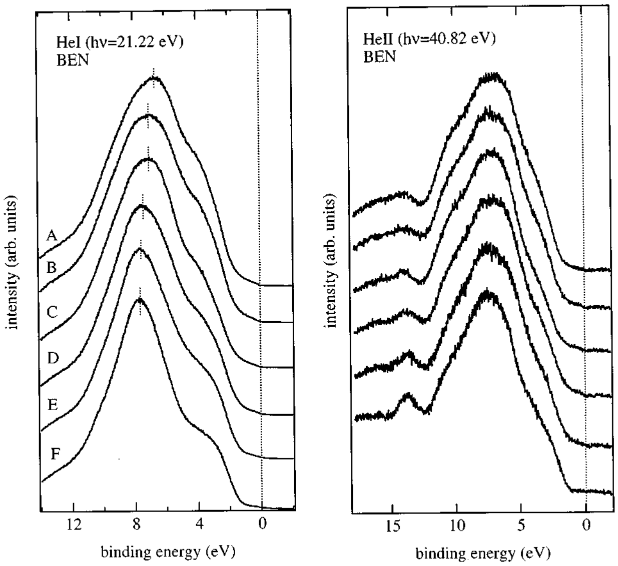

FIG. 1. Temporal evolution of the UPS-VB spectra [He I (left) and He II (right)] excitation in the course of the BEN pretreatment period. The spectra are shown in order of increasing deposition time from top (3 min) to bottom (15 min).

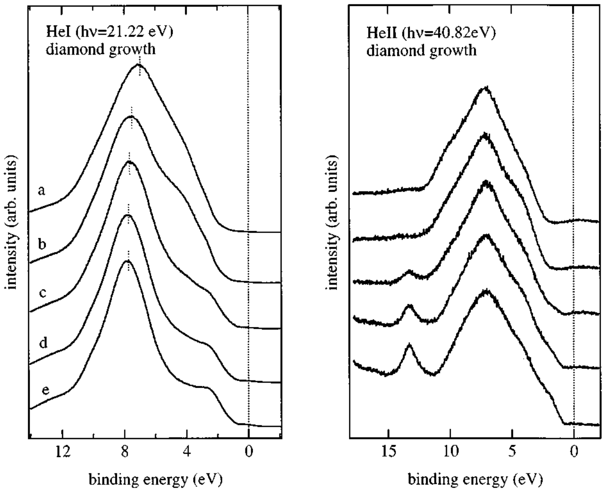

FIG. 2. Temporal evolution of the UPS-VB spectra [He I (left) and He II (right) excitation] in the course of the diamond growth period. The spectra are shown in order of increasing deposition time from top (0.5 min) to bottom (15 min). A BEN period of 9 min preceded the diamond growth in this case.

binding energies of about 2.5–3.0 eV gains in intensity. In the He II VB spectra the same general evolution of the spectral shape is observed, with the exception of a small peak at 13.7 eV binding energy, which is well defined for deposition times exceeding 7.5 min. The general shape of the spectra recorded for short deposition times is very similar to the ones observed for various forms of amorphous carbon.[19–22] The appearance of two overlapping and rather broad peaks is attributable to the excitation of photoelectrons from the p-σ and p-π bands, respectively. These bands are formed by p electrons which participate in chemical bonds of either σ or π symmetry and dominate the UPS spectra on account of their larger excitation cross section as compared to the lower-lying bands with predominantly s character.[23] In contrast to the spectra of amorphous carbon the ones of graphite or films containing large graphitic clusters are dominated by a number of narrow peaks which are related to direct transitions in the band structure of graphite.[24] The size of graphitic clusters which already exhibit VB spectra very similar to graphite was estimated by Schelz[18] to be around 2.5 nm, which amounts to about 300–500 carbon atoms in a graphitic cluster.

The VB spectra obtained for long deposition times show a considerable reduction in the contributions from the p-π band and the width of the main peak at 7.7 eV and bear already a strong similarity to the VB spectrum of diamond.[25,26] The shoulder which now appears at about 3 eV stems from surface states on a partially reconstructed diamond surface and is retained for the diamond film achieved after completion of the deposition (Fig. 2). It is, however, somewhat surprising that these states are already observed at this point of the deposition process. A study dealing with the interaction of carbon with the diamond surface is currently under way and might enable us to resolve this question. The additional peak in the He II spectra at 13.7 eV is likewise characteristic for diamond and has its origin in the excitation from a narrow band of mixed s and p character in the band structure of diamond.[27,28] These observations strongly suggest the presence of diamond as well as an amorphous carbon phase during the BEN pretreatment period. There is no indication for the presence of graphite or numerous large graphitic clusters. However, apart from the pure carbon phases a contribution from SiC (formed at the substrate-carbon film interface) to the VB spectra has to be considered. A comparison with VB spectra of SiC, which are described in the literature,[29] shows that the carbide phase does not contribute significantly to the VB spectra obtained for the BEN films. This point will be addressed in more detail later on in connection with the results obtained for the diamond growth step and the MXPS analysis.

We proceed now with the deposition of diamond following a BEN pretreatment period of 9 min. The resulting VB spectra as a function of diamond deposition time are depicted in Fig. 2. Beginning with the film obtained after the 9-min BEN period we observe a shift of the main peak to lower binding energies of 7.0 eV, followed by an upward shift to 7.7±0.1 eV. At the same time the position of the valence-band maximum E_v with respect to the Fermi energy E_F increases in the first diamond deposition step, but is reduced again for subsequent deposition periods and a shoulder located at about 2.7 eV gains in intensity. In the He II spectra a similar development is observed and the characteristic diamond peak at 13.5 eV is well defined albeit still low in intensity for the early deposition steps. Its intensity with respect to the main peak increases in the course of the last deposition steps. The width of the main peak in the He I as well as the He II excited VB spectra is reduced considerably with increasing deposition time and the spectra obtained after 15 min are those well known from polycrystalline diamond films and described in detail by Francz and Oelhafen.[25]

The spectrum obtained after only 30 sec of diamond deposition differs from the amorphous carbon as well as the diamond spectra and does most likely contain a substantial contribution from a silicon carbide or carbon enriched silicon carbide phase. This claim is supported by a comparison with

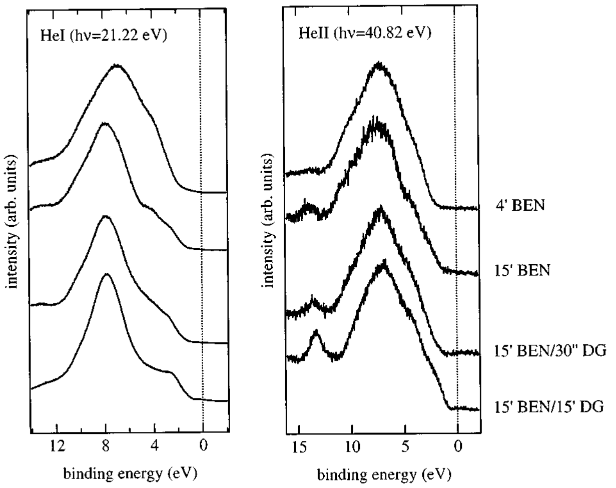

FIG. 3. UPS-VB spectra [He I (left) and He II (right) excitation] or carbon/diamond films formed in a deposition cycle with an extended BEN period of 15 min. The respective deposition times are indicated in the figure.

data on the SiC valence-band spectra given in the literature[29] and also by the information gained from the analysis of the C 1*s* and Si 2*p* core levels, which is described in the following paragraphs. Specifically the shift in position of the most intense peak, the shape of the low-binding-energy side of this peak, and the shift in the position of E_v from 1.6 (BEN, 9 min) to 1.9 eV (BEN, 9 min plus diamond growth, 0.5 min) support this interpretation.

The same general development of the film structure during the deposition process is observed if we chose an extended pretreatment time of 15 min and a different plasma adjustment which results in higher deposition rates during BEN. A selection of VB spectra for this series is shown in Fig. 3. Again we observe the deposition of an amorphous carbon phase at the beginning of BEN and a decrease in the contribution from p-π states as well as an increasing contribution from diamond. This development continues after switching to the diamond deposition after 15 min BEN, and after 15 min of diamond growth the typical diamond spectrum is obtained. For this series, however, contributions from a carbide phase are not apparent in the UPS spectra owing to the extended BEN pretreatment period.

These results are in agreement with the information on the film structure which can be deduced from the electron energy loss spectroscopy. The loss spectrum is at the beginning of BEN dominated by a peak located at 23 eV with respect to the primary beam energy (500 eV), which can stem either from an amorphous carbon phase or SiO_2.[30] During the BEN period the emergence of the characteristic diamond plasmon at 34 eV is observed and after the subsequent diamond growth period a typical loss spectrum of diamond is obtained. As has been reported earlier,[13] the intensity of the π-π^* shakeup peak located at 5.5–6.0 eV is very low, which is indicative of a film structure with only small contributions from aromatic rings or graphitic clusters. Although this points toward the presence of an amorphous sp^3-carbon-rich network, the plasmon peak which is typical for the dense ta-C phase and located at about 30 eV is not observed. It should, however, be noted that the detection limit for a minority component with EELS is in our experience around 5–10 %, a number which is also given by Belton and Schmieg.[15] Complementary to the information from the UPS spectra an analysis of the C 1*s* and Si 2*p* core-level lines provides information about the local chemical bonding of the elements. The results for the C 1*s* core level, which correspond to the series of films for which the UPS spectra are shown in Fig. 2, are depicted in Fig. 4 as a function of deposition time for the BEN [Fig. 4(a)] and the diamond growth [Fig. 4(b)] periods.

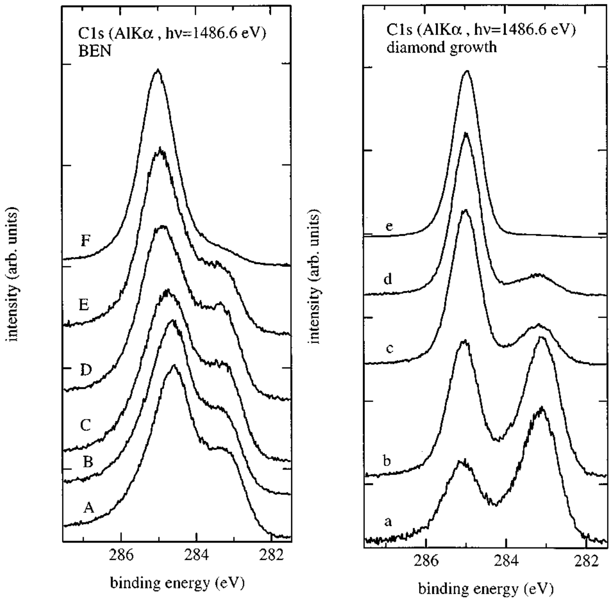

FIG. 4. Temporal evolution of the carbon 1*s* core level (MXPS, Al $K\alpha$) in the course of the BEN pretreatment period (left-hand side) and the diamond growth period (right-hand side). The spectra are shown in order of increasing deposition time from bottom to top. A BEN period of 9 min preceded the diamond growth period.

For the C 1*s* core level two distinct peaks are observed which are located at $284.6+0.3$ and 283.3 ± 0.1 eV, respectively, and stem from carbon which forms a homonuclear bond (C-C) as in diamond, amorphous carbon, or graphite, and the silicon carbide phase, respectively. The carbon peak is continuously shifted to higher binding energies during the BEN period and it gains in intensity with respect to the carbide peak for deposition times exceeding 12 min. Switching to diamond deposition conditions we observe a considerable decrease in the half-width and the intensity of the carbon peak (Figs. 4 and 5). The contribution from the carbon phase peak increases with deposition time and after 15 min the carbide peak is barely perceptible and the typical symmetric diamond C 1*s* peak has emerged (Fig. 4).

On account of the large half-width of the C 1*s* peak for the BEN films the respective concentrations of differently bonded carbon atoms cannot be determined by a simple integration procedure but a deconvolution of the core-level peak is required. However, a proper deconvolution of the C 1*s* peak poses a number of challenges and questions which have yet to be resolved.[15] Unlike for metals, where extensive research in recent years has led to a much improved understanding of the photoemission process and the corresponding line shapes of the core-level peaks,[31] the behavior of most

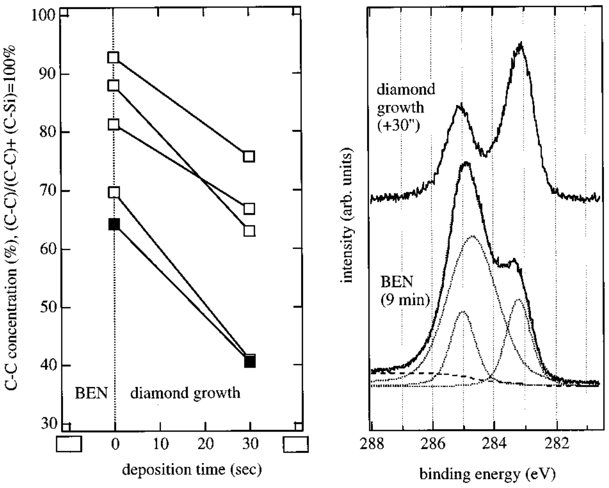

FIG. 5. Changes in the surface concentration of carbon which forms homonuclear (C-C) bonds upon switching from BEN to diamond growth conditions. The concentration is determined by a deconvolution procedure which allows a separation of carbon and carbide contributions. An example for a deconvolution is given on the right-hand side of the figure and the C 1*s* spectra correspond to the concentrations marked with a filled symbol. Assignment: continuous lines: spectra as measured; dotted lines: peaks obtained from the deconvolution; broken line: Shirley background.

insulators is still only poorly understood. We are aware of the fact that therefore our deconvolution as described below has to be rather rudimentary and it will mainly be used to extract information on the relative concentration of the carbide and carbon phases.

A deconvolution of the C 1*s* core-level peak using symmetric Doniach-Sunjic functions[32] leads only to a satisfactory result if we assume that at least two peaks contribute to the carbon phase peak and a third one can clearly be attributed to the SiC phase. For the carbide peak we only observe changes in its intensity; the half-width as well as the peak position remain constant throughout the whole deposition period (BEN and diamond growth). On the other hand, considerable changes in the shape of the carbon phase peak are observed. Regarding the position of the carbon phase peak (or its components), however, unfortunately does not allow an unequivocal assignment of the components since it is strongly influenced by a number of different effects such as surface band bending, crystallite orientation, amorphicity, and sp^2/sp^3 ratio.[15,33]

The deconvolution suggests that the two majority components are distinguished by their Gaussian half-widths, which are 1.5 ± 0.2 and 0.8 ± 0.1 eV. The Lorentzian contribution, on the other hand, is determined by the lifetime of the core hole and can be assumed to be largely independent of the chemical environment of the carbon atom. In agreement with the literature a Lorentzian half-width[34,35] of 0.3 eV was used for all carbon core-level peaks. Fluctuations in the near or medium range order caused by bond angle and bond length distortions are known to lead to a broadening of the core-level peaks in amorphous materials, e.g., amorphous silicon or amorphous carbon. Throughout the deposition it is observed that the peak with a smaller half-width of 0.8 ± 0.1 eV gains in intensity with respect to the broader peak, which disappears after switching to diamond growth conditions. An example for the deconvolution is included in Fig. 5. We conclude from the temporal evolution and a comparison with the spectrum obtained after the first diamond growth step that the narrow peak originates from the diamond phase while the broader peak is attributable to an amorphous phase. This is at the same time in excellent agreement with information obtained from the analysis of the UPS spectra.

The oxygen concentration at the surface is below 2.0% during the BEN pretreatment and reaches its highest level of about 6% upon switching to diamond growth conditions. The oxygen concentration is again reduced to levels below 2% for increasing lengths of the diamond growth period. This illustrates the presence of highly reactive surfaces with probably a large number of dangling bonds, especially during the early stages of the diamond growth period. The oxygen appears to be attached to the Si or the SiC of the interface, leading to the formation of a mixed SiO_xC_y phase. This can be deduced from a slight broadening of the Si 2*p* peak on the high-binding-energy side of the main peak.[36] We can expect that the composition of the SiO_xC_y component is rather poorly defined and therefore no distinct peak with a well-defined chemical shift with respect to the main carbide peak can be distinguished unequivocally.

The most dramatic changes with respect to the C 1*s* core-level peak, the relative surface concentration of the carbon phase, and the UPS spectra occur immediately after switching from the BEN pretreatment to the deposition conditions appropriate for diamond growth. Even a rather brief interval of only 30 sec of diamond growth is sufficient to trigger considerable changes in the film structure and composition. The change in the concentration of the carbon phase was investigated for various pretreatment intervals (6–15 min) and plasma adjustments and the results are summarized in Fig. 5. The reduction in the concentration of the carbon phase is apparently independent of the deposition conditions; it lies between 18% and 30% and is generally less pronounced for higher initial concentrations. The example for the deconvolution of the C 1*s* peak included in this figure also shows that the peak component assigned earlier to an amorphous carbon phase disappears in the early stages of the diamond growth period. Except for this brief time interval the carbon concentration increases during the BEN pretreatment as well as during the diamond growth period continuously.

Following this detailed discussion of the film composition and structure we will now turn our attention to the evolution of the interfacial region between the growing carbon film and the silicon substrate. The Si 2*p* core-level spectra are depicted in Fig. 6 as a function of deposition time for the BEN [Fig. 6(a)] and the diamond growth [Fig. 6(b)] periods and belong to the same deposition series as the C 1*s* and UPS spectra discussed earlier. In all spectra two majority components can be identified, which are centered at 99.6 and 100.6 eV, and can be attributed to silicon and SiC, respectively. A deconvolution of the Si 2*p* peak yields the concentration of silicon carbide with respect to elemental silicon and the results are summarized in Fig. 7. In the course of the BEN pretreatment the carbide contribution remains unchanged, while during the diamond growth period a continuous decrease from 60% to about 25% is observed. If the formation

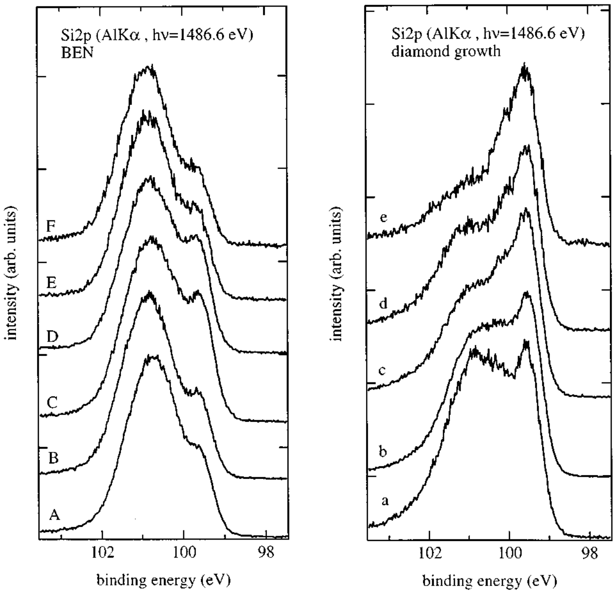

FIG. 6. Temporal evolution of the silicon $2p$ core level (MXPS, Al $K\alpha$) in the course of the BEN pretreatment period (left-hand side) and the diamond growth period (right-hand side). The spectra are shown in order of increasing deposition time from bottom to top. A BEN period of 9 min preceded the diamond growth period.

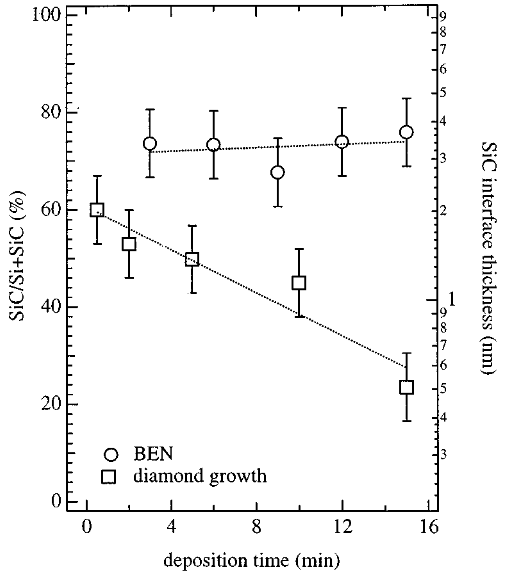

FIG. 7. Concentration of SiC as a function of the deposition time for the BEN and the diamond growth period. The thickness of the SiC overlayer (right axis) was calculated using Eq. (2). The dotted line is a least-squares fit to the data.

of a homogeneous carbide layer is assumed, the measured carbide concentration with respect to the contribution from the underlying substrate is directly related to the interface thickness. The attenuation of the photoelectron current I_0 passing through a layer of material with a thickness x is described by

$$I(x)=I_0\exp\left(-\frac{x}{l}\right), \tag{1}$$

with l as the inelastic mean free path of the photoelectrons. According to Seah and Dench[37] the mean free path amounts to about 2.0 nm for excitation energies around 1500 eV as they are provided by an Al $K\alpha$ source. The interface thickness d is then related to the ratio of the intensities I of the SiC and Si contributions to the Si $2p$ core-level peak by the following equation:

$$d=\ln\left(\frac{I(\mathrm{SiC})}{I(\mathrm{Si})}+1\right) l. \tag{2}$$

The interface thickness remains constant with about 3.5 nm during the BEN period and is reduced considerably to 2.0 nm and then to about 0.5 nm in the course of the diamond growth period (Fig. 7). It can be concluded, that a carbide interface of maximum thickness is formed in the early stages of the BEN period and subsequently removed partially during the diamond growth period.

DISCUSSION

The experimental results described in detail in the preceding section enable us to develop a qualitative model for the mechanism of the BEN pretreatment, which is supported by all spectroscopic methods applied in the current study. During the BEN period the codeposition of diamond and an amorphous carbon phase as well as the formation of a SiC interface are observed. A graphite or predominantly graphitic phase apparently does not participate in this growth process, and the absence of considerable contributions from this phase is confirmed by UPS and EELS. The contribution of the crystalline diamond phase to the carbon deposit on the surface increases with the BEN deposition time, which indicates an increasing crystallite size and/or nuclei density. An analysis of the BEN deposit with scanning electron microscopy (SEM) shows the presence of roundish, ballas-type crystals lacking well-defined facets,[38] whose size and number increase significantly with the deposition time. We can now safely assume that these poorly defined crystals are indeed to a large extent composed of diamond. These overcritical diamond nuclei subsequently serve as growth centers for the formation of the polycrystalline diamond film.

The codeposition of an amorphous carbon phase is triggered through the ion irradiation during the BEN pretreatment. The ion energies involved are certainly below 100 eV (Refs. 7 and 9) and their penetration depth in the growing film is therefore restricted to a few angstroms.[8] The energies of the ions are nonetheless sufficient to cause bond breakage, enhance the surface diffusion of adsorbed species, and introduce structural disorder in a shallow surface layer. On the other hand, the plasma chemistry, especially the high concentration of atomic hydrogen, is favorable for the formation of diamond.[39] The interplay of these two factors favors the codeposition of amorphous carbon and diamond.

Upon switching from BEN to diamond growth conditions the irradiation with energetic ions ceases and the amorphous carbon phase is to a large extent removed through etching by atomic hydrogen (see Fig. 5). The diamond nuclei are, on the other hand, stable and continue to grow unhindered. The instability of amorphous carbon in a hydrogen-rich environment has been shown by Olson *et al.*[39] in an experiment, which involved the sequential deposition of carbon and its exposure to hydrogen. The ion irradiation during BEN is therefore crucial to sustain the amorphous phase. The benefit of BEN is apparently to provide an environment which promotes nucleation through the formation of a carbon phase, which grows easily under these deposition conditions. The presence of a carbon phase other than diamond appears to be the decisive factor which enables us to achieve the dramatic increase in nucleation densities as compared to other methods.

In view of the classical nucleation theories[40] the codeposition of the amorphous phase might supply the necessary local supersaturation in order to trigger the nucleation of the crystalline phase. At the same time an amorphous layer provides numerous defects which can again serve as local nucleation centers and certainly changes in the adsorbed species mobility on the surface also cannot be neglected. The ion irradiation during BEN would then only be required to deposit a thin carbon layer which serves as a mold for the formation of critical diamond nuclei. A different model suggests that the subplantation[8] of ions leads to the formation of an overdense region just below the surface of the carbon film and therefore drives the nucleation of diamond. Both models disagree on the driving force of diamond nucleation, but are commensurate with the experimental results presented in this study.

Some additional information on the microstructure of the amorphous carbon phase can be gained from the UPS and EELS analysis and by comparison with other amorphous phases which have been prepared by electron-beam evaporation or ion-beam deposition techniques. In the VB spectra a contribution from the p-π band, albeit smaller than usually observed for electron-beam evaporated carbon, is readily apparent. The amorphous carbon phase formed during the BEN period does not contain large graphitic clusters or olefinic chains, since the VB and the EELS spectra both lack the typical features associated with extended π-bonded or graphitic systems, respectively. The appearance of a p-π band is, however, incompatible with the presence of a pure ta-C which has been suggested to act as a nucleation enhancing layer. Following the data presented here, we suggest that the amorphous carbon phase formed during BEN is a strongly cross-linked network formed of sp^2 and sp^3 carbon without extended graphitic regions but in which the diamond nuclei are embedded. The presence of large amounts of hydrogen cannot be discounted from our PES analysis, since PES is insensitive to hydrogen, but appears unlikely in the light of other investigations on the hydrogen evolution from amorphous hydrogenated carbon (a-C:H) films.[41]

The carbide interface is formed already in the very early stages of the BEN pretreatment and its thickness, deduced from the ratio of silicon to silicon carbide, remains unchanged throughout the pretreatment step. It is unaffected by the continuing film growth and the ion irradiation, but switching to diamond growth conditions leads to a dramatic decrease in the carbide concentration and therefore the thickness of the interfacial layer. A part of the protective layer composed of amorphous carbon and the diamond nuclei has been removed under diamond growth conditions and the carbide is now directly exposed to high fluxes of atomic hydrogen. This could also lead to a carbide layer of uneven thickness, since the layer which is located beneath the diamond nuclei might remain mostly unaffected. This observation is also in agreement with our results on the removal of the amorphous carbon phase through etching and the carbon layer can be pictured as a mold of amorphous carbon in which the diamond nuclei are embedded.

CONCLUSIONS

The experiment described here combines the *in situ* deposition of diamond films and their analysis with photoelectron spectroscopy, namely, UPS and MXPS, and EELS. The observation of the temporal evolution of the film growth during the BEN pretreatment as well as the diamond growth period lead us to a concise description of the nucleation process. In the course of the BEN pretreatment an amorphous carbon phase of as yet uncertain microstructure as well as the crystalline diamond phase are codeposited. The plasma conditions and low-energy ion irradiation during BEN support the codeposition of both phases. The formation of the amorphous phase is obviously beneficial for the nucleation of diamond, although the underlying mechanism remains to be determined. If the low-energy ion irradiation is turned off and plasma conditions supportive of good quality diamond growth are chosen, the amorphous carbon phase is removed by etching through the interaction with atomic hydrogen. A SiC layer is formed in the early stages of the deposition process and is unaffected by the continuing pretreatment, but its thickness is reduced considerably by etching during the diamond growth period.

ACKNOWLEDGMENTS

The authors wish to thank R. Steiner for his technical support. We also gratefully acknowledge the financial support of the present work by the Swiss Priority Program on Materials Research carried out under the auspices of the trinational ''D-A-CH'' cooperation involving Germany, Austria, and Switzerland on the ''Synthesis of Superhard Materials.''

---

[1] Z. Feng, K. Komvopoulos, I. G. Brown, and D. B. Bogy, J. Appl. Phys. **74**, 2841 (1993).

[2] X. Jiang, K. Schiffmann, and C.-P. Klages, Phys. Rev. B **50**, 8402 (1994).

[3] B. R. Stoner, G.-H. Ma, S. D. Wolter, and J. T. Glass, Phys. Rev. B **45**, 11 067 (1992).

[4] S. Yugo, T. Kanai, T. Kimura, and T. Muto, J. Appl. Phys. **58**, 1036 (1991).

[5] B. R. Stoner and J. T. Glass, Appl. Phys. Lett. **60**, 699 (1992).

[6] X. Jiang and C. Lia, Appl. Phys. Lett. **67**, 1197 (1995).

[7] J. Gerber, M. Weiler, O. Sohr, K. Jung, and H. Ehrhardt, Diam. Relat. Mater. **3**, 506 (1994).

[8] Y. Lifshitz, S. R. Kasi, and J. W. Rabalais, Phys. Rev. Lett. **62**, 1290 (1989).

[9] S. P. McGinnis, M. A. Kelly, and S. B. Hagström, Appl. Phys. Lett. **66**, 3117 (1995).

[10] P. Reinke, J. E. Klemberg-Sapieha, and L. Martinu, J. Appl. Phys. **76**, 5754 (1994).

[11] S. Geier, R. Hessmer, U. Preckwinkel, D. Schweitzer, M. Schreck, and B. Rauschenbach, J. Appl. Phys. **79**, 1907 (1996).

[12] S. P. McGinnis, M. A. Kelly, S. B. Hagström, and R. L. Alvis, J. Appl. Phys. **79**, 170 (1996).

[13] P. Reinke, P. Kania, P. Oelhafen, and R. Guggenheim, Appl. Phys. Lett. **68**, 22 (1996).

[14] W. R. L. Lambrecht, C. H. Lee, B. Segall, J. C. Angus, Z. Li, and M. Sunkara, Nature (London) **364**, 607 (1993).

[15] D. N. Belton and S. J. Schmieg, J. Vac. Sci. Technol. A **8**, 2353 (1990).

[16] F. R. McFeely, S. P. Kowalczyk, L. Ley, R. G. Cavell, R. A. Pollak, and D. A. Shirley, Phys. Rev. B **9**, 5268 (1974).

[17] J. Schäfer, J. Ristein, R. Graupner, L. Ley, U. Stephan, T. Fraunheim, V. S. Veerasany, G. A. J. Amaratunga, M. Weiler, and H. Ehrhardt, Phys. Rev. B **53**, 7762 (1996).

[18] S. Schelz, P. Kania, P. Oelhafen, H.-J. Güntherodt, and T. Richmond, Surf. Sci. **359**, 227 (1995).

[19] P. Oelhafen, D. Ugolini, S. Schelz, and J. Eitle, in *Diamond and Diamond-like Films and Coatings*, Vol. 266 of *NATO Advanced Study Institute, Series B: Physics*, edited by R. E. Clausing, L. H. Horton, J. C. Angus, and P. Koidl (Plenum, New York, 1992).

[20] P. Reinke and P. Oelhafen, J. Appl. Phys. **81**, 2396 (1997).

[21] J. Schäfer, J. Ristein, and L. Ley, Diam. Relat. Mater. **3**, 861 (1994).

[22] D. Ugolini, J. Eitle, and P. Oelhafen, Vacuum **41**, 1374 (1990).

[23] A. Bianconi, S. B. M. Hagström, and R. Z. Bachrach, Phys. Rev. B **16**, 5543 (1977).

[24] A. Zunger, Phys. Rev. B **17**, 626 (1978).

[25] G. Francz and P. Oelhafen, Diam. Relat. Mater. **4**, 539 (1995).

[26] J. Ristein and R. Graupner, Adv. Solid State Phys. **36**, 77 (1996).

[27] G. S. Painter, D. E. Ellis, and A. R. Lubinsky, Phys. Rev. B **4**, 3610 (1971).

[28] F. J. Himpsel, J. F. v. d. Veen, and D. E. Eastman, Phys. Rev. B **22**, 1967 (1980).

[29] R.-C. Fang and L. Ley, Phys. Rev. B **40**, 3818 (1989).

[30] J. Fink, T. M. Heinzerling, J. Pflüger, B. Scheerer, B. Dischler, P. Koidl, A. Bubenzer, and R. E. Sah, Phys. Rev. B **30**, 4713 (1984).

[31] S. Hüfner, in *Photelectron Spectroscopy*, edited by M. Cardona, P. Fulde, K. von Klitzing, and H.-J. Queisser, Springer Series in Solid State Sciences Vol. 82 (Springer, Berlin, 1995).

[32] S. Doniach and M. Sunjic, J. Phys. C **3**, 285 (1970).

[33] G. Francz and P. Oelhafen, Surf. Sci. **329**, 193 (1995).

[34] F. Sette, G. K. Wertheim, Y. Ma, G. Meigs, S. Modessi, and C. T. Chen, Phys. Rev. B **41**, 9766 (1990).

[35] G. Francz (private communication).

[36] S. Schelz and P. Oelhafen, Surf. Sci. **279**, 137 (1992).

[37] M. P. Seah and W. A. Dench, Surf. Interface Anal. **1**, 2 (1979).

[38] P. Reinke, P. Kania, and P. Oelhafen, Thin Solid Films **270**, 124 (1995).

[39] D. S. Olson, M. A. Kelly, S. Kapoor, and S. B. Hagstrom, J. Appl. Phys. **74**, 5167 (1993).

[40] C. H. L. Goodman, *Crystal Growth-Theory and Techniques* (Plenum, London, 1974).

[41] C. Wild and P. Koidl, in *Amorphous Hydrogenated Carbon Films*, edited by P. Koidl and P. Oelhafen (Les Editions de Physique, Les Ulis, 1987), Vol. 17, p. 207.